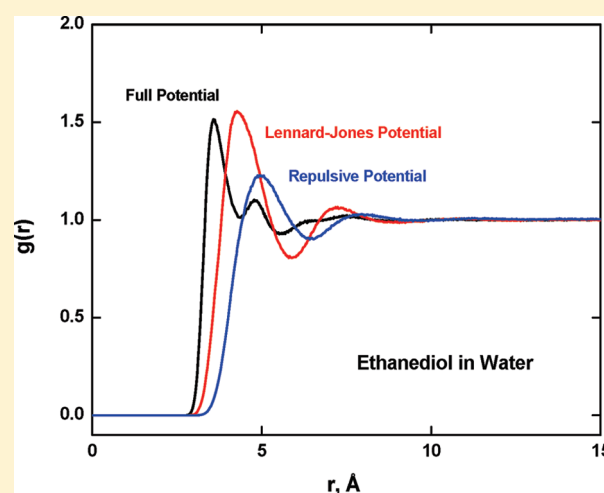


# Parsing Partial Molar Volumes of Small Molecules: A Molecular Dynamics Study

Nisha Patel,<sup>†</sup> David N. Dubins,<sup>†</sup> Régis Pomès,<sup>‡</sup> and Tigran V. Chalikian<sup>\*,†</sup><sup>†</sup>Department of Pharmaceutical Sciences, Leslie Dan Faculty of Pharmacy, University of Toronto, 144 College Street, Toronto, Ontario M5S 3M2, Canada<sup>‡</sup>Molecular Structure and Function Programme, Hospital for Sick Children, and Department of Biochemistry, University of Toronto, Toronto, Canada

**ABSTRACT:** We used molecular dynamics (MD) simulations in conjunction with the Kirkwood–Buff theory to compute the partial molar volumes for a number of small solutes of various chemical natures. We repeated our computations using modified pair potentials, first, in the absence of the Coulombic term and, second, in the absence of the Coulombic and the attractive Lennard–Jones terms. Comparison of our results with experimental data and the volumetric results of Monte Carlo simulation with hard sphere potentials and scaled particle theory-based computations led us to conclude that, for small solutes, the partial molar volume computed with the Lennard–Jones potential in the absence of the Coulombic term nearly coincides with the cavity volume. On the other hand, MD simulations carried out with the pair interaction potentials containing only the repulsive Lennard–Jones term produce unrealistically large partial molar volumes of solutes that are close to their excluded volumes. Our simulation results are in good agreement with the reported schemes for parsing partial molar volume data on small solutes. In particular, our determined interaction volumes and the thickness of the thermal volume for individual compounds are in good agreement with empirical estimates. This work is the first computational study that supports and lends credence to the practical algorithms of parsing partial molar volume data that are currently in use for molecular interpretations of volumetric data.



## INTRODUCTION

The partial molar volume,  $V^\circ$ , of a solute is the pressure derivative of its chemical potential. As such, it is a fundamental thermodynamic property reflecting the entire spectrum of inter- and intramolecular interactions of a solute, including solute–solvent interactions commonly referred to as solvation. Interpretation of partial molar volume data and, ultimately, the usability of such data for characterizing changes in hydration associated with various biological processes depend on the model used to link the measured macroscopic observables with solute–solvent interactions. The scheme that has been used most widely for parsing partial molar volume data is based on the relationship<sup>1</sup>

$$V^\circ = V_C + V_I + \beta_{T_0}RT \quad (1)$$

where  $V_C$  is the volume of the cavity enclosing a solute in the absence of attractive solute–solvent interactions;  $V_I$  is the interaction volume;  $\beta_{T_0}$  is the coefficient of isothermal compressibility of the solvent;  $R$  is the universal gas constant; and  $T$  is the absolute temperature. The cavity volume can be viewed as consisting of the region occupied by the solute and an “empty” border region between the solute and the unaltered, uniform

pure solvent.<sup>2,3</sup> In this scheme, the region occupied by the solute is its intrinsic volume,  $V_M$ , while the empty border region is the thermal volume,  $V_T$ ;  $V_C = V_M + V_T$ . Note that the  $V_C$  and  $V_I$  terms of eq 1 reflect the volume change due to the addition of a solute molecule at a fixed position in the solvent, while the translational  $\beta_{T_0}RT$  term originates from the availability of the entire volume of the solution to the solute.

The intrinsic volume,  $V_M$ , is the geometric volume of the solute that is impenetrable to surrounding water molecules. The  $V_T$  is the operationally defined void volume created around a solute molecule due to the mutual vibrations of solute and solvent molecules as well as to structural, packing, and steric effects. The interaction volume,  $V_I$ , represents reduction of the solvent volume under the influence of direct solute–solvent interactions. Significantly,  $V_I$  is the only component of the partial molar volume,  $V^\circ$ , of a solute directly reflecting its solvation. Evaluation of  $V_I$  requires estimation of the  $V_M$  and  $V_T$  components of the cavity volume,  $V_C$ , in eq 1. The intrinsic volume of a

Received: February 8, 2011

Revised: March 15, 2011

Published: April 05, 2011

solute can be evaluated in a relatively straightforward manner as the molecular volume, that is, the volume enclosed within the molecular surface of a solute.<sup>4,5</sup> For a small solute,  $V_M$  can be approximated by its van der Waals volume,  $V_W$ . The latter can be calculated additively based on the chemical structure of a solute and the van der Waals volume group contributions.<sup>6,7</sup> Clearly, the situation is more complicated for the biopolymers proteins and nucleic acids in which case the intrinsic volume depends on the conformation of the macromolecule.<sup>8</sup>

Determination of the thermal volume,  $V_T$ , is less straightforward and currently based on purely empirical approaches. In one approach, the cavity volume,  $V_C$ , of a solute is a linear function of its van der Waals volume,  $V_W$ ;  $V_C = aV_W + b$ , where  $a = 1.53$  and  $b = 9.9 \text{ cm}^3 \text{ mol}^{-1}$  for hydrocarbons.<sup>9</sup> In an alternative approach, the thermal volume,  $V_T$ , of a nonpolar molecule consists of a layer of “empty” volume of a constant thickness,  $\delta$ .<sup>1,10</sup> With this assumption and the spherical approximation of a solute, the cavity volume is given by the relationship

$$V_C = \left(\frac{4\pi N_A}{3}\right)(r + \delta)^3 \quad (2)$$

where  $N_A$  is Avogadro's number and  $r = (3V_W/4\pi N_A)^{1/3}$  is the radius of the approximating sphere.

The thickness of the void volume,  $\delta$ , has been empirically estimated to be between 0.50 and 0.57 Å.<sup>1,10</sup> These estimates agree with the calculations based on scaled particle theory (SPT), a simple theory in which the solute and solvent molecules are approximated by hard spheres.<sup>1,11</sup> These empirical schemes have proven useful and have been extensively employed in rationalizing partial molar volume data on various solutes. However, the veracity of such rationalizations and the hydration pictures that they produce remain untested in the absence of more rigorous theoretical verifications.

Most importantly, the practical evaluation of the cavity volume,  $V_C$ , is possible only for nonpolar molecules for which the interaction volume,  $V_I$ , can be neglected (see eq 1). Thus, eq 2 can be applied to evaluating the thickness,  $\delta$ , of the thermal volume,  $V_T$ , of nonpolar but not polar solutes. For a solute containing polar and/or charged groups and, therefore, exhibiting a nonzero value of  $V_I$ , the cavity volume,  $V_C$ , can be estimated under the assumption that  $\delta$  does not depend on the chemical nature of the solute.<sup>1</sup> In other words, it is assumed that  $\delta$  is the same for polar and nonpolar solutes, independently of their chemical composition and size.<sup>1</sup> This assumption forms the basis of molecular interpretations of partial molar volume data on solutes or changes in volume accompanying various chemical processes (e.g., binding reactions and conformational transitions of biopolymers) has never been tested in any rigorous theoretical way. This deficiency is serious, since it undermines the veracity of insights derived from volumetric investigations of biophysical and biochemical systems.

In acknowledgment of this deficiency, we combined in this work molecular dynamics (MD) simulations with the Kirkwood–Buff (KB) theory to compute the partial molar volume of a number of polar and nonpolar solutes and to parse the resulting partial molar volumes into their intrinsic, thermal, and interactions components. Specifically, we applied MD simulations to calculating the solute–solvent radial distribution functions (RDF) that were subsequently used in conjunction with the KB theory to compute the partial molar volumes of various solutes. The MD simulations were performed with three solute–solvent pair interaction potentials. First, we used the full pair

interaction potentials  $U_{ij} = 4\epsilon_{ij}[(\sigma_{ij}/r)^{12} - (\sigma_{ij}/r)^6] + q_i q_j / (4\pi\epsilon_0\epsilon r)$  to compute the RDF and the partial molar volume of a solute. Second, we carried out MD simulations and volume calculations for the same solute with modified pair potentials that are limited to the Lennard-Jones terms,  $U_{ij} = 4\epsilon_{ij}[(\sigma_{ij}/r)^{12} - (\sigma_{ij}/r)^6]$  and do not contain the Coulombic contribution. Finally, we repeated the computations with pair potentials containing only the repulsive Lennard-Jones term,  $U_{ij} = 4\epsilon_{ij}(\sigma_{ij}/r)^{12}$ . Comparison of the partial molar volumes obtained with the three different pair potentials enabled us to extract and analyze the  $V_M$ ,  $V_T$ , and  $V_I$  contributions in eq 1.

## METHODS

**Molecular Dynamic Simulations.** The MD simulations were carried out with the GROMACS software, version 4.0.5.<sup>12</sup> The solutes were modeled based on the OPLS-AA parametrization.<sup>13</sup> Water was modeled using the TIP3P potential which, despite its simplicity, quantifies the structural and thermodynamic properties of water with a reasonably high accuracy.<sup>14</sup> Each simulation box consisted of 2176 TIP3P water molecules and one solute molecule in a cubic cell with the edge of 40.0 Å with periodic boundary conditions applied. The Lennard-Jones interactions were evaluated out to a separation of 12 Å and smoothly switched to zero at a cutoff distance of 15 Å. Long-range electrostatic interactions were evaluated using particle mesh Ewald method<sup>15</sup> with a real-space cutoff of 15 Å and a Fourier grid spacing of 1.2 Å.

The MD simulations were carried out in the isothermal–isobaric NPT ensemble for all solutes in water at the temperature of 298 K (Nose–Hoover thermostat) and the pressure of 1 atm (Parinello–Rahman ensemble)<sup>16–18</sup> using the leapfrog algorithm with a time step of 0.002 ps. All bonds were constrained using LINCS.<sup>19</sup> The steepest descent method was used to perform 500 steps of energy minimization to ensure relaxation of the system. This step was followed by two-phase equilibration runs using the weak coupling technique.<sup>20</sup> Initially, a 100 ps equilibration run was implemented in the canonical NVT ensemble to thermalize the system at 298 K. This was followed by the second 1 ns run in the isothermal–isobaric NPT ensemble to equilibrate the system at 1 atm and 298 K. The final production run of 100 ns was performed with configurations saved every 2 ps for analysis. Errors were estimated as the standard deviation of the mean from block averaging over 20 ns for each production run. The resulting MD trajectories were used to compute the solute–solvent RDFs between the center of mass of each solute and the oxygen atoms of water.

**Determination of Partial Molar Volumes via the Kirkwood–Buff Integrals.** The KB theory is an exact statistical mechanical theory that links RDFs,  $g_{ij}(r)$ , in the grand canonical ensemble ( $\mu$ VT) with the derivatives of the chemical potentials of the species in the system.<sup>21–25</sup> These properties are expressed via the KB integral,  $G_{ij}$ , between the species  $i$  and  $j$

$$G_{ij} = G_{ji} = \int_0^\infty [g_{ij}^{\mu VT}(r) - 1] 4\pi r^2 dr \quad (3)$$

In the limit of infinite dilution, the partial molar volume of a solute is related to the solute–solvent KB integral via the expression<sup>24,25</sup>

$$V^\circ = -G_{12} + \beta_{T_0} RT \quad (4)$$

The KB integral reflects the average excess (or deficiency) of  $j$  particles around the central  $i$  particle relative to the random distribution in an equivalent volume of the bulk solution. Note

that this expression cannot be applied to the canonical NVT ensemble in which case the KB integrals trivially yield either 0 or  $-1$ .<sup>25</sup> We calculated the KB integrals from our simulated RDFs using the following approximation<sup>26–29</sup>

$$G_{ij} = \int_0^{\infty} [g_{ij}^{\text{NVT}}(r) - 1] 4\pi r^2 dr$$

$$\approx \int_0^{R'} [g_{ij}^{\text{NPT}}(r) - 1] 4\pi r^2 dr \quad (5)$$

where  $R'$  is the extent of the integration beyond which the RDF approaches unity, that is, the bulk solution value.

The partial molar volumes were determined at the integration cutoff distances,  $R'$ , of 10, 12, and 15 Å. We found no statistically significant differences between the partial molar volumes calculated with the cutoff distances of 12 and 15 Å. Consequently, the cutoff of 12 Å was chosen as the standard for the computation of the partial molar volumes of the solutes. The choice of this cutoff is further justified by our selected cutoff radius for the calculation of Lennard-Jones interactions which is also 12 Å (see above).

In practice, computation of KB integrals is complicated due to the noisiness and long-range oscillations of simulated RDFs that do not converge to unity unless extended simulation boxes (with dimensions exceeding several diameters of the solute molecule) are considered. Although the deviation of RDFs from unity is small (on the order of  $1/N$  in a closed system), the influence of this deviation on the KB integral may be very significant due to the factor  $r^2$  in the integrand of eq 5.<sup>30</sup> Several algorithms have been proposed to circumvent this problem by normalizing RDFs in NPT and NVT ensembles. In particular, in the hydration shell model, it has been proposed that the entire contribution to the local component of the partial molar volume of a solute originates from the first hydration shell with the contributions of the more distant shells canceling each other.<sup>31</sup> Elsewhere, the RDFs have been normalized by using water density computed in a region of a solution far from the solute,<sup>32</sup> by averaging the integral over a short distance range (typically, one molecular diameter),<sup>26,29</sup> and by introducing a screening radius which enhances the convergence of KB integral in such a way that it essentially reaches its asymptotic limit within the first hydration shell.<sup>33</sup>

Here, we introduce the following procedure to enhance the convergence of the KB integrals. We compute the KB integral by averaging the  $g(r)$  function beyond the truncation distance of 12 Å and substituting the obtained average as the asymptotic limit in the KB integral in place of unity (see eq 5). The deviation from unity of the average value of  $g(r)$  beyond 12 Å was on the order of  $\pm 0.0001$ . This procedure enhances the convergence of the KB integral by smoothing the oscillations in the RDFs.

**Direct Determination of Partial Molar Volumes.** The partial molar volume of a solute can be also determined following the direct algorithm as described by Moghaddam and Chan.<sup>34</sup> In the direct method, the partial molar volume of a solute is computed as the difference in the ensemble average volumes between two NPT boxes, one containing solvent and a single solute molecule and the other containing pure solvent at the same temperature and pressure. The ensemble average volume,  $\langle V \rangle$ , for each NPT box was derived from MD simulations. The difference between the two ensemble averages is equal to the partial molar volume of a solute.

## RESULTS AND DISCUSSION

**Partial Molar Volumes. Comparison with Experimental Data.** Table 1 lists the partial molar volumes,  $V^\circ$ , for a number of

**Table 1. Partial Molar Volumes of Solutes<sup>a</sup>**

solute	KB cm <sup>3</sup> mol <sup>-1</sup>	DM cm <sup>3</sup> mol <sup>-1</sup>	EX cm <sup>3</sup> mol <sup>-1</sup>
methane	38.8 ± 1.0	37.7 ± 1.2	37.3 <sup>b</sup>
ethane	54.3 ± 0.7	55.1 ± 1.5	51.2 <sup>b</sup>
benzene	85.1 ± 0.9	87.7 ± 2.2	83.1 <sup>b</sup>
water	18.0 ± 0.1	18.3 ± 0.8	18.07
methanol	39.1 ± 1.8	38.5 ± 2.6	38.2 <sup>b</sup>
ethanol	53.7 ± 0.9	55.1 ± 2.7	55.1 <sup>b</sup>
1,2-ethanediol	52.9 ± 1.2	55.2 ± 1.3	54.6 <sup>b</sup>
ammonia	26.9 ± 0.4	25.6 ± 1.8	24.8 <sup>b</sup>
urea	40.9 ± 0.5	39.5 ± 0.9	44.2 <sup>b</sup>
glycine (zwitterionic)	32.6 ± 1.1	31.7 ± 1.8	43.3 <sup>c</sup>
glycine (neutralized)	55.1 ± 1.1	56.5 ± 2.2	56.2 <sup>d</sup>
alanine (zwitterionic)	48.0 ± 1.2	45.8 ± 1.1	60.4 <sup>c</sup>
alanine (neutralized)	70.2 ± 1.2	72.7 ± 2.2	73.5 <sup>e</sup>
lithium (Li+)	-10.9 ± 1.0	3.2 ± 1.4	-11.2 <sup>f</sup> , -6.6 <sup>g</sup>
sodium (Na+)	-7.5 ± 0.6	6.5 ± 1.4	-7.4 <sup>f</sup> , -6.9 <sup>g</sup>
chloride (Cl-)	23.1 ± 1.2	10.9 ± 1.0	23.7 <sup>f</sup> , 23.5 <sup>g</sup>
bromide (Br-)	27.8 ± 0.9	14.9 ± 1.7	30.2 <sup>f</sup> , 30.4 <sup>g</sup>

<sup>a</sup> KB, calculated with eq 4; DM, evaluated from the direct method; EX, experimental values. <sup>b</sup> From ref 1. <sup>c</sup> From ref 41. <sup>d</sup> The partial molar volume of glycolamide, an uncharged isomer of glycine.<sup>44</sup> <sup>e</sup> The partial molar volume of lactamide, an uncharged isomer of alanine.<sup>45</sup> <sup>f</sup> From ref 46. <sup>g</sup> From ref 47.

solutes, including charged, polar, and nonpolar organic compounds as well as inorganic ions, calculated with the KB theory (second column) and the direct method (DM) (third column). The two data sets are in good agreement with each other with the exception of the four inorganic ions. The large discrepancies between the KB and DM values observed in Table 1 for single ions (whereby the partial molar volume is overestimated by DM for the cations and underestimated for the anions) probably reflect artifacts due to Ewald summation in a system with a net total charge. Note that this discrepancy vanishes in the case of ion pairs (results not shown), for zwitterionic systems (see Table 1), and in the absence of Coulombic interactions (see Table 2).

Figure 1 compares our partial molar volumes computed using KB theory with the reported experimental data (the latter are listed in the fourth column of Table 1). The comparison reveals that our computed partial molar volumes are consistent with experimental data for most of the solutes with the exception of the two zwitterionic amino acids. The reason for the disparity is not clear but may be related to the conformational dependence of electronic polarization of both solvent and solute molecules in the electrostatic field of the charged termini of zwitterionic glycine and alanine that is neglected in the force field used in our MD simulations. This effect compounds the assumption of transferability of partial-charge parameters developed for small ionic fragments to a zwitterionic molecule. In contrast, our calculated partial molar volumes of glycine and alanine with neutralized termini agree well with the partial molar volumes of glycolamide and lactamide (uncharged isomers of glycine and alanine), respectively. The observed agreement between the calculated and experimental partial molar volumes of the predominant majority of the solutes investigated in this work lends credence to our calculations and the subsequent analysis.

**Simulations Carried out without the Coulombic Term.** Figure 2 depicts representative RDFs of methanol (panel a),



**Table 2.** Partial Molar Volumes of Solutes Computed from MD Simulations with the Lennard-Jones Potential via the KB Integrals (KB) and the Direct Method (DM) and with the Repulsive Lennard-Jones Potential Only (RLJ) via the KB Integrals<sup>a</sup>

solute	KB cm <sup>3</sup> mol <sup>-1</sup>	DM cm <sup>3</sup> mol <sup>-1</sup>	SPT <sup>b</sup> cm <sup>3</sup> mol <sup>-1</sup>	literature <sup>c</sup> cm <sup>3</sup> mol <sup>-1</sup>	RLJ cm <sup>3</sup> mol <sup>-1</sup>
methane	39.2 ± 0.7	39.3 ± 1.6	36.6	34.6	78.0 ± 0.8
ethane	54.1 ± 0.7	56.4 ± 0.8	53.0	50.9	115.4 ± 0.3
benzene	85.7 ± 1.0	88.7 ± 1.5	84.9	82.2	201.1 ± 1.2
water	29.0 ± 1.0	27.5 ± 1.0	28.7	26.2	
methanol	44.2 ± 0.9	45.2 ± 2.3	44.3	42.3	95.3 ± 1.0
ethanol	60.3 ± 0.6	62.2 ± 1.8	60.2	58.1	132.9 ± 1.2
1,2-ethanediol	64.5 ± 1.7	66.8 ± 1.9	67.3	65.8	148.3 ± 1.1
ammonia	34.7 ± 1.0	33.8 ± 1.2	29.9	29.0	61.7 ± 0.5
urea	51.8 ± 1.2	55.5 ± 1.3	55.9	58.2	168.2 ± 0.6
glycine	64.0 ± 0.7	66.8 ± 2.4	72.9		
alanine	80.3 ± 0.9	84.3 ± 0.6	88.1		
lithium (Li <sup>+</sup> )	11.8 ± 0.6	10.8 ± 0.8			
sodium (Na <sup>+</sup> )	24.7 ± 0.8	23.5 ± 0.7			
chloride (Cl <sup>-</sup> )	55.8 ± 1.2	57.5 ± 1.9			
bromide (Br <sup>-</sup> )	61.2 ± 0.9	63.6 ± 1.4			

<sup>a</sup> Cavity volumes computed from SPT (SPT) and reported empirical schemes (literature). <sup>b</sup> In SPT calculations of cavity volume,<sup>36</sup> each solute was approximated by a sphere with a radius of  $r = (3V_W/4\pi N_A)^{1/3}$ , where  $V_W$  is its van der Waals volume. The hard sphere radius of a water molecule used in the calculations is 1.37 Å.<sup>1,11</sup> <sup>c</sup> From ref 1.

ethanol (panel b), and 1,2-ethanediol (panel c) computed with the full pair potentials (black lines) and the Lennard-Jones pair interaction potentials in the absence of the Coulombic term (red lines). The second and third columns of Table 2 present the partial molar volumes of the solutes calculated with the Lennard-Jones potentials in the absence of the Coulombic term. As mentioned above, the large discrepancies between the KB and DM values observed in Table 1 for single ions disappear once the simulations are performed in the absence of Coulombic interactions (see Table 2).

Data presented in Table 2 correspond to hypothetical analogs that have the same geometry but lack the charges that may be present in real solutes; in other words, the nonpolar analogs of the solutes. A comparison of data listed in Tables 1 and 2 reveals that in agreement with conventional wisdom the two calculation modes (with and without the Coulombic potential) yield similar partial molar volumes for the nonpolar solutes methane, ethane, and benzene. In contrast, for solutes containing polar and/or charged groups, calculations performed with the full pair potentials produce lower partial molar volumes than those performed without the Coulombic term. The disparity reflects solvent contraction in the vicinity of polar and charged groups due to solute–solvent hydrogen bonding and electrostriction.

**To a Good Approximation, the Partial Molar Volume of a Solute Devoid of All Charges Equals Its Cavity Volume.** Monte Carlo simulations with hard-sphere potentials in conjunction with the KB integrals have been used to compute the volumes of spherical cavities with radii of up to 8.6 Å.<sup>35</sup> This approach should arguably produce the closest approximation of the cavity volume. The results of Monte Carlo simulations have been compared with the cavity volumes calculated with SPT, another hard-sphere theory albeit less sophisticated.<sup>35</sup> SPT, in which the solute and solvent molecules are approximated by hard spheres, has been extensively employed for calculating the cavity volumes for various solutes.<sup>2,36</sup> For hard-sphere cavities with diameters of less than ~4 Å, the results of the Monte Carlo and SPT calculations nearly coincide.<sup>35</sup> However, for larger cavities,

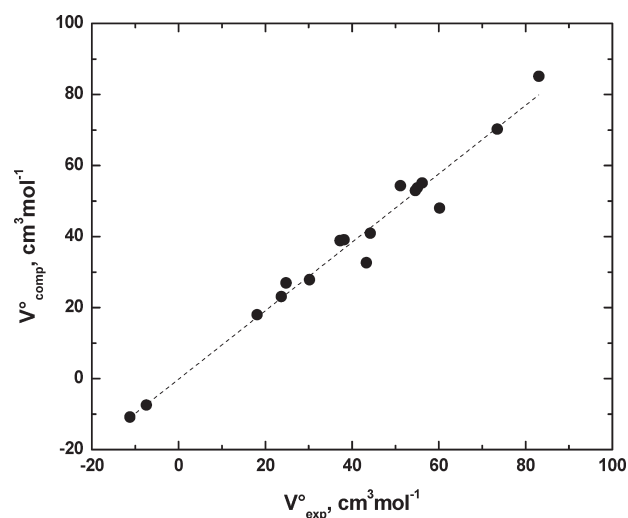


**Figure 1.** Partial molar volumes,  $V_{\text{comp}}^{\circ}$ , of the solutes computed based on the KB theory plotted versus experimental values,  $V_{\text{exp}}^{\circ}$  (from Table 1). Errors for the calculated values are comparable to the size of the symbols.

the volumes calculated from the Monte Carlo simulations increasingly deviate from those calculated by means of SPT.<sup>35</sup> The observed deviation may partly reflect the approximate nature of SPT and, partly, dewetting of large nonpolar surfaces in water,<sup>37</sup> a feature detected by Monte Carlo simulations but not by SPT.

Monte Carlo simulations with hard sphere potentials and SPT-based computations can be readily performed on model spherical cavities. However, simulations on real solutes are problematic due to the ambiguity related to assigning specific hard sphere diameters to solutes or their constituent atoms or atomic groups. Nonetheless, SPT-based calculations of the partial molar volumes of small nonpolar solutes produce results

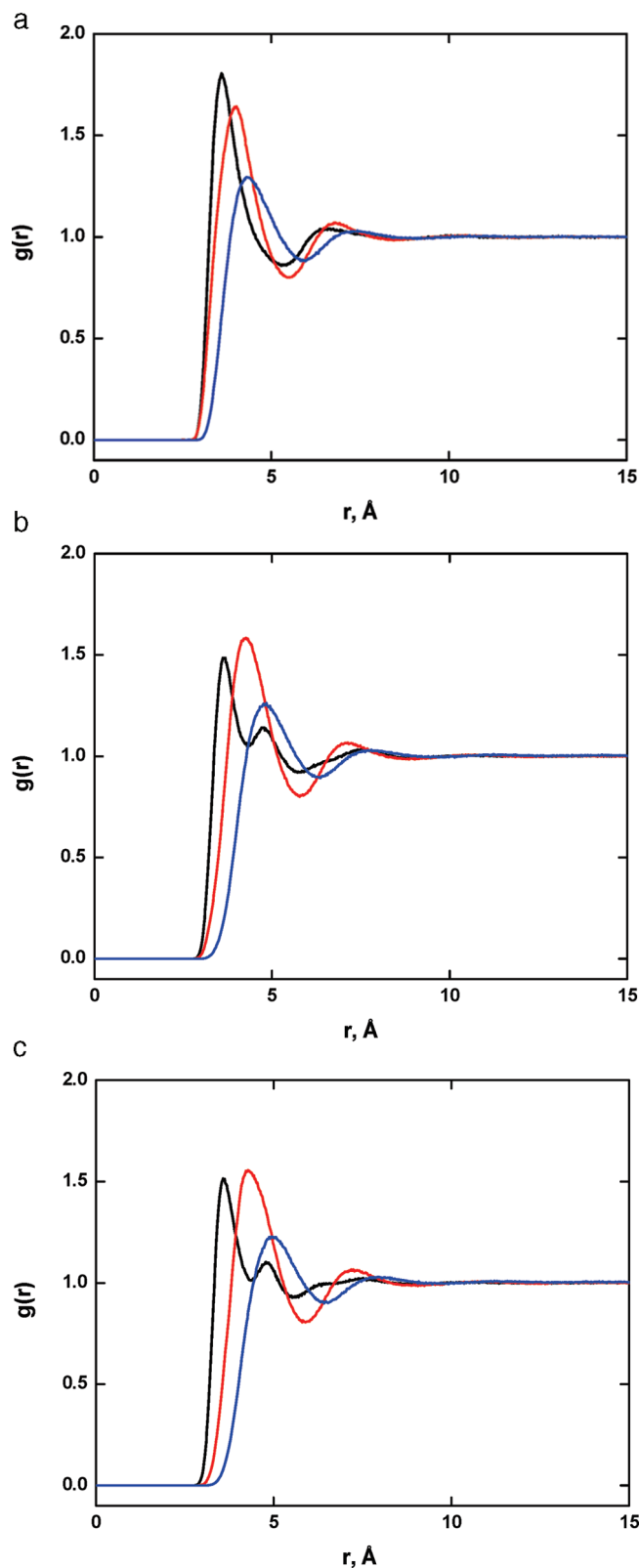


**Figure 2.** Solute–solvent radial distribution functions between the center of mass of a solute and the oxygen atom of water for methanol (panel a), ethanol (panel b), and 1,2-ethanediol (panel c) computed with the full pair potentials (black lines), the Lennard-Jones pair interaction potentials in the absence of the Coulombic  $q_i q_j / (4\pi\epsilon_0 \epsilon r)$  term (red lines), and the repulsive Lennard-Jones potential only (blue lines).

that are in impressive agreement with experimental values.<sup>2</sup> In particular, the thickness of the thermal volume,  $\delta$ , determined empirically from the partial molar volume data on nonpolar solutes<sup>10</sup> is nearly identical to that determined from SPT-based simulations.<sup>1,2,11</sup> On the basis of these agreements, it is plausible to expect that the partial molar volume of nonpolar solutes is predominantly determined by their cavity volumes. Our simulation results listed in Table 2 are consistent with this expectation; the partial molar volumes of solutes computed with Lennard-Jones potential in the absence of the Coulombic term (“nonpolar” volumes) are in good agreement with those we calculated with SPT. We performed the SPT calculations of partial molar volumes as described previously<sup>36</sup> using a hard sphere radius for a water molecule of 1.37 Å.<sup>1,11</sup> The hard sphere radii,  $r$ , for the solutes were evaluated from the van der Waals volumes,  $V_W$ , based on the spherical approximation,  $r = (3V_W/4\pi N_A)^{1/3}$ .

Recall that cavity volume refers to the partial molar volume of a hard core solute (which does not interact with its surrounding water molecules by any attractive forces) minus the translational  $\beta_{T_0} RT$  term. The attractive  $(\sigma_{ij}/r)^6$  term of the Lennard-Jones potential may, therefore, influence the “nonpolar” volume of a solute. To estimate the magnitude of this influence, we repeated our calculations with the pair potential containing only the repulsive Lennard-Jones term,  $U_{ij} = 4\epsilon_{ij}(\sigma_{ij}/r)^{12}$ . The computed RDFs for methanol (panel a), ethanol (panel b), and 1,2-ethanediol (panel c) are shown in Figure 2 (marked in blue). The partial molar volumes for a set of selected solutes calculated with the repulsive Lennard-Jones potential are listed in the sixth column of Table 2. Inspection of the data presented in Table 2 reveals that the partial molar volumes of solutes calculated with the repulsive potential are significantly larger than those calculated with the full Lennard-Jones potential. In fact, the partial molar volume of a solute calculated with the repulsive potential is so great that it is close to the excluded volume. The latter is defined as the volume encompassed within the solvent accessible surface of a solute, that is, the surface traced out by the center of a spherical probe of a radius of 1.4 Å as it rolls over the surface of the solute (the excluded volume is larger than the cavity volume of a solute). This result suggests that, in the absence of the neutralizing influence of the attractive  $(\sigma_{ij}/r)^6$  term, the repulsive  $4\epsilon_{ij}(\sigma_{ij}/r)^{12}$  potential extends to unrealistically large distances from the central solute. In other words, as far as partial molar volume is concerned, the repulsive  $4\epsilon_{ij}(\sigma_{ij}/r)^{12}$  potential is a poor substitute for the hard sphere potential.

In the aggregate, our computed partial molar volumes of nonpolar analogs of the solutes coincide with SPT-based calculations which, in turn, are consistent with Monte Carlo simulations with hard sphere potentials.<sup>35</sup> This observation suggests that the nonpolar volume of a small solute, independent of its chemical nature, is a good approximation of the cavity volume,  $V_C$ . It also lends credence to the practical algorithms for parsing the partial molar volumes of solutes reported in the literature.<sup>1,9,10</sup> In particular, our computational results support the validity of the empirical approach in which the thermal volume,  $V_T$ , is calculated as a layer of void space of a constant thickness that does not depend on the chemical nature of the solute.<sup>1</sup>

**Thermal Volume and the Thickness of the Void Volume.** Thermal volume,  $V_T$ , can be viewed as consisting of a layer of void volume surrounding the solute. To estimate the thickness of the thermal volume,  $\delta$ , we approximate the solutes by spheres. Alternatively, instead of a sphere one can use a set of simple

**Table 3.** van der Waals ( $V_W$ ) and Interaction ( $V_I$ ) Volumes ( $\text{cm}^3 \text{mol}^{-1}$ ) and the thicknesses of thermal volume ( $\delta$ , Å) of the Solutes<sup>a</sup>

solute	$V_W \text{ cm}^3 \text{ mol}^{-1}$	$\delta \text{ \AA}$	$V_I \text{ cm}^3 \text{ mol}^{-1}$	literature $\text{cm}^3 \text{ mol}^{-1}$
methane	17.1 <sup>b</sup>	0.51	$-0.4 \pm 1.4$	1.6 <sup>d</sup>
ethane	27.3 <sup>b</sup>	0.48	$0.2 \pm 1.0$	$-0.8^d$
benzene	48.4 <sup>b</sup>	0.47	$-0.6 \pm 0.6$	$-0.2^d$
water	12.0 <sup>b</sup>	0.49	$-10.9 \pm 0.5$	$-9.3^d$
methanol	21.7 <sup>b</sup>	0.46	$-5.2 \pm 2.1$	$-5.1^e; -5.2^d$
ethanol	31.9 <sup>b</sup>	0.46	$-6.6 \pm 0.7$	$-3.7^e; -4.7^d$
1,2-ethanediol	36.5 <sup>b</sup>	0.43	$-11.6 \pm 1.9$	$-12.3^d$
ammonia	13.7 <sup>b</sup>	0.54	$-7.8 \pm 0.7$	$-5.3^d$
urea	32.8 <sup>b</sup>	0.33	$-10.9 \pm 1.0$	$-15.1^d$
glycine (zwitterionic)			$-31.4 \pm 1.4$	$-27.0^f; -24.1^g$
glycine (neutralized)	40.5 <sup>b</sup>	0.39	$-12.1 \pm 1.1$	
alanine (zwitterionic)			$-32.3 \pm 1.6$	
alanine (neutralized)	50.7 <sup>b</sup>	0.40	$-12.0 \pm 1.3$	
lithium ( $\text{Li}^+$ )	3.2 <sup>c</sup>	0.48	$-22.6 \pm 1.1$	$-16.3^h$
sodium ( $\text{Na}^+$ )	11.6 <sup>c</sup>	0.59	$-32.2 \pm 1.2$	$-17.3^h$
chloride ( $\text{Cl}^-$ )	27.4 <sup>c</sup>	0.59	$-32.7 \pm 1.1$	$-11.5^h$
bromide ( $\text{Br}^-$ )	30.3 <sup>c</sup>	0.60	$-33.4 \pm 1.3$	$-11.0^h$

<sup>a</sup> Reported empirical estimates of interaction volumes (literature) and the thickness of the thermal volume,  $\delta$ . <sup>b</sup>  $V_W$  was calculated according to Bondi.<sup>6</sup> <sup>c</sup>  $V_W$  was calculated using the McVol algorithm.<sup>38</sup> <sup>d</sup> Reference 1. <sup>e</sup> Reference 9. <sup>f</sup> Reference 41. <sup>g</sup> Reference 40. <sup>h</sup> Reference 43.

three-dimensional geometric figures approximating the shape of a solute molecule.<sup>1</sup> However, approximation of a solute by a nonspherical shape does not necessarily translate into a higher accuracy of the determination of thermal volume due to a large number of adjustable geometric parameters.

With the spherical approximation, the cavity volume of a solute is given by eq 2. For all solutes but the inorganic ions, we calculated the  $V_W$  required for determining the hard sphere radii,  $r = (3V_W/4\pi N_A)^{1/3}$ , in eq 2 using the additive approach presented by Bondi.<sup>6</sup> In this procedure, each solute is conceptually divided into constituent atomic groups with  $V_W$  being computed as the sum of respective group contributions reported by Bondi.<sup>6</sup> Such an additive scheme is valid for the low molecular weight solutes studied in this work, although these molecules exhibit flexibility around their covalent bonds. Given their small size, the conformational space sampled by these solutes should overwhelmingly consist of fully solvent-accessible conformations with negligible nonadditive effects. The situation is more complicated for larger molecules that may exhibit conformations with internal voids formed by partially or fully buried atomic groups. The van der Waals volumes of the inorganic ions were computed using the Monte Carlo-based algorithm McVol.<sup>38</sup>

Our calculated van der Waals volumes,  $V_W$ , for the solutes studied here are listed in the second column of Table 3. Note that our calculated van der Waals volume of an isolated water molecule is  $12.0 \text{ cm}^3 \text{ mol}^{-1}$  (the contribution of a hydroxyl group is  $8.04 \text{ cm}^3 \text{ mol}^{-1}$ , while the average contribution of a hydrogen atom is  $\sim 4 \text{ cm}^3 \text{ mol}^{-1}$ ).<sup>6</sup> This volume is larger than that of a hydrogen-bonded water molecule of  $6.9 \text{ cm}^3 \text{ mol}^{-1}$  as evaluated based on the "hydrogen-bonded" radius of a water molecule of  $\sim 1.4 \text{ \AA}$ .

The values of  $\delta$  calculated with eq 2 are presented in the third column of Table 3. Our computed values of  $\delta$  ranging from 0.4 to  $0.6 \text{ \AA}$  are in good agreement with the empirical estimates reported in literature.<sup>1,2,10</sup>

**Interaction Volumes.** The interaction volume,  $V_I$ , of charged and polar molecules in water is due to electrostriction and/or

formation of solute–solvent hydrogen bonding.<sup>1,9,39</sup> Thus, solutes will display negative  $V_I$  according to their charge, polarity, and hydrogen bonding capability. We calculated the values of  $V_I$  for each solute as the difference between its  $V^\circ$  and the sum of the cavity volume,  $V_C$ , and the ideal term  $\beta_{T_0}RT$  (see eq 1). The calculated values of  $V_I$  are listed in the fourth column of Table 3.

Inspection of data in Table 3 reveals that in agreement with conventional wisdom the interaction volume,  $V_I$ , for the non-polar solutes we studied (the alkanes and benzene) is close to zero. On the other hand, strongly polar groups such as hydroxyl or amino groups that can form up to three hydrogen bonds with water molecules exhibit large negative values of  $V_I$ . For example, methanol and ethanol are characterized by interaction volumes of  $-5.2$  and  $-6.6 \text{ cm}^3 \text{ mol}^{-1}$ , respectively, in good agreement with empirical estimates.<sup>1,9</sup> 1,2-Ethanediol with its two hydroxyl groups is characterized by a  $V_I$  of  $-11.6 \text{ cm}^3 \text{ mol}^{-1}$ , twice as negative as those of methanol and ethanol. It has been empirically estimated that the formation of a solute–solvent hydrogen bond causes on average a volume contraction of about  $2.2 \text{ cm}^3 \text{ mol}^{-1}$ .<sup>11</sup> Thus, the average number of solute–water hydrogen bonds can be roughly estimated for a solute by dividing its  $V_I$  by  $-2.2 \text{ cm}^3 \text{ mol}^{-1}$ .

For the ions and the zwitterionic amino acids studied here, the hydration shell is predominantly formed under the influence of strong charge-dipole interactions between the solute and water. For these solutes, the interaction volumes,  $V_I$ , are strongly negative, which reflects electrostriction of the solvent by the charges. Note that our determined value of  $V_I$  for glycine is in qualitative agreement with previously reported empirical estimates.<sup>40,41</sup> In contrast, our results on  $V_I$  for the ions are significantly more negative than the previous SPT-based theoretical estimates.<sup>42,43</sup>

The interaction volume,  $V_I$ , calculated for glycine and alanine with neutralized termini (equal to  $-12.1$  and  $-12.0 \text{ cm}^3 \text{ mol}^{-1}$ , respectively) reflect the formation of solute–solvent hydrogen bonds in the absence of electrostriction. The differential  $V_I$  for the amino acids with the ionized and neutralized termini reflects

the contribution of electrostriction that roughly equals  $-20 \text{ cm}^3 \text{ mol}^{-1}$ .

In general, inspection of data presented in Table 3 reveals a good agreement between our computed  $V_I$  and the reported empirical estimates (the fifth column). This agreement further supports the reliability of the reported practical approaches used for microscopic rationalization of volumetric data.

## CONCLUSION

We used MD simulations in conjunction with the KB theory to compute the partial molar volumes for a number of small solutes of various chemical natures. Our calculated partial molar volumes are in good agreement with the experimental data. Additionally, the partial molar volumes of the same solutes were computed using modified pair potentials. First, we carried out MD simulations using the Lennard-Jones potential in the absence of the Coulombic term. Second, the simulations were performed with the pair potential containing only the repulsive Lennard-Jones term. Simulations performed with the full Lennard-Jones potential yield for the small molecules studied here partial molar volumes that are in close agreement with the cavity volumes derived from calculations with scaled particle theory (SPT). Given this observation and the fact that for solutes with a diameter of less than  $\sim 4 \text{ \AA}$  the cavity volumes calculated with SPT are similar to those computed with Monte Carlo simulations with hard sphere potentials,<sup>35</sup> we conclude that the cavity volume,  $V_C$ , of a small molecule nearly coincides with its nonpolar volume. The latter is the partial molar volume of a solute devoid of its charges that can be computed from MD simulations using the Lennard-Jones potential in the absence of the Coulombic term. On the other hand, MD simulations carried out with the repulsive Lennard-Jones term produce unrealistically large partial molar volumes of solutes that are close to their excluded volumes. This result suggests that the repulsive Lennard-Jones potential is a poor substitute for the hard sphere potential. In general, our theoretical results are in good agreement with the derivations based on practical approaches to parsing partial molar volume data on small solutes. In particular, our determined interaction volume,  $V_I$ , and the thickness of the thermal volume,  $\delta$ , for individual solutes are consistent with the empirical estimates. To the best of our knowledge, this work is the first computational study that supports and lends credence to the empirical algorithms of parsing partial molar volume data.

## AUTHOR INFORMATION

### Corresponding Author

\*Tel: (416)946-3715. Fax: (416)978-8511. E-mail: chalikan@phm.utoronto.ca.

## ACKNOWLEDGMENT

This work was supported by an NSERC Grant to T.V.C. R.P. is a CRCP chairholder. The authors thank the SciNet Consortium for a generous allocation of CPU resources.

## REFERENCES

- (1) Kharakoz, D. P. *J. Solution Chem.* **1992**, *21*, 569–595.
- (2) Lee, B. J. *Phys. Chem.* **1983**, *87*, 112–118.
- (3) Graziano, G. *Chem. Phys. Lett.* **2006**, *429*, 420–424.
- (4) Richards, F. M. *Annu. Rev. Biophys. Bioeng.* **1977**, *6*, 151–176.
- (5) Richards, F. M. *Methods Enzymol.* **1985**, *115*, 440–464.
- (6) Bondi, A. J. *Phys. Chem.* **1964**, *68*, 441–451.
- (7) Edward, J. T. *J. Chem. Educ.* **1970**, *47*, 261–270.
- (8) Chalikian, T. V.; Filfil, R. *Biophys. Chem.* **2003**, *104*, 489–499.
- (9) Terasawa, S.; Itsuki, H.; Arakawa, S. *J. Phys. Chem.* **1975**, *79*, 2345–2351.
- (10) Edward, J. T.; Farrell, P. G. *Can. J. Chem.* **1975**, *53*, 2965–2970.
- (11) Likhodi, O.; Chalikian, T. V. *J. Am. Chem. Soc.* **1999**, *121*, 1156–1163.
- (12) van der Spoel, D.; Lindahl, E.; Hess, B.; Groenhof, G.; Mark, A. E.; Berendsen, H. J. C. *J. Comput. Chem.* **2005**, *26*, 1701–1718.
- (13) Jorgensen, W. L.; Maxwell, D. S.; Tirado-Rives, J. *J. Am. Chem. Soc.* **1996**, *118*, 11225–11236.
- (14) Jorgensen, W. L.; Chandrasekhar, J.; Madura, J. D.; Impey, R. W.; Klein, M. L. *J. Chem. Phys.* **1983**, *79*, 926–935.
- (15) Darden, T.; York, D.; Pedersen, L. *J. Chem. Phys.* **1993**, *98*, 10089–10092.
- (16) Nose, S. *Mol. Phys.* **1984**, *52*, 255–268.
- (17) Hoover, W. G. *Phys. Rev. A* **1985**, *31*, 1695–1697.
- (18) Parrinello, M.; Rahman, A. *J. Appl. Phys.* **1981**, *52*, 7182–7190.
- (19) Hess, B.; Bekker, H.; Berendsen, H. J. C.; Fraaije, J. G. E. M. *J. Comput. Chem.* **1997**, *18*, 1463–1472.
- (20) Berendsen, H. J. C.; Postma, J. P. M.; Vangunsteren, W. F.; Dinola, A.; Haak, J. R. *J. Chem. Phys.* **1984**, *81*, 3684–3690.
- (21) Kirkwood, J. G.; Buff, F. P. *J. Chem. Phys.* **1951**, *19*, 774–777.
- (22) Hall, D. G. *Trans. Faraday Soc.* **1971**, *67*, 2516–2524.
- (23) Ben-Naim, A. *J. Chem. Phys.* **1975**, *63*, 2064–2073.
- (24) Ben-Naim, A. *Statistical Thermodynamics for Chemists and Biochemists*; Plenum Press: New York, 2002.
- (25) Ben-Naim, A. *Molecular Theory of Solutions*; Oxford University Press: Oxford, 2006.
- (26) Weerasinghe, S.; Smith, P. E. *J. Phys. Chem. B* **2003**, *107*, 3891–3898.
- (27) Weerasinghe, S.; Smith, P. E. *J. Chem. Phys.* **2004**, *121*, 2180–2186.
- (28) Smith, P. E. *J. Phys. Chem. B* **2004**, *108*, 18716–18724.
- (29) Weerasinghe, S.; Smith, P. E. *J. Phys. Chem. B* **2005**, *109*, 15080–15086.
- (30) Lebowitz, J. L.; Percus, J. K. *Phys. Rev.* **1961**, *122*, 1675–1691.
- (31) Matubayasi, N.; Levy, R. M. *J. Phys. Chem.* **1996**, *100*, 2681–2688.
- (32) Lin, C. L.; Wood, R. H. *J. Phys. Chem.* **1996**, *100*, 16399–16409.
- (33) Lockwood, D. M.; Rosicky, P. J. *J. Phys. Chem. B* **1999**, *103*, 1982–1990.
- (34) Moghaddam, M. S.; Chan, H. S. *J. Chem. Phys.* **2007**, *126*, 114507.
- (35) Floris, F. M. *J. Phys. Chem. B* **2004**, *108*, 16244–16249.
- (36) Pierotti, R. A. *Chem. Rev.* **1976**, *76*, 717–726.
- (37) Chandler, D. *Nature* **2005**, *437*, 640–647.
- (38) Till, M. S.; Ullmann, G. M. *J. Mol. Model.* **2010**, *16*, 419–429.
- (39) Shahidi, F.; Farrell, P. G.; Edward, J. T. *J. Chem. Soc., Faraday Trans. I* **1977**, *73*, 715–721.
- (40) Chalikian, T. V.; Sarvazyan, A. P.; Breslauer, K. J. *J. Phys. Chem.* **1993**, *97*, 13017–13026.
- (41) Kharakoz, D. P. *Biophys. Chem.* **1989**, *34*, 115–125.
- (42) Hirata, F.; Arakawa, K. *Bull. Chem. Soc. Jpn.* **1973**, *46*, 3367–3369.
- (43) Hirata, F.; Imai, T.; Irida, M. *Rev. High Pressure Sci. Technol.* **1998**, *8*, 96–103.
- (44) Gucker, F. T.; Ford, W. L.; Moser, C. E. *J. Phys. Chem.* **1939**, *43*, 153–168.
- (45) Gucker, F. T.; Allen, T. W. *J. Am. Chem. Soc.* **1942**, *64*, 191–199.
- (46) Zana, R.; Yeager, E. *J. Phys. Chem.* **1967**, *71*, 521–536.
- (47) Conway, B. E. *J. Solution Chem.* **1978**, *7*, 721–770.